# Mass-Resolved Infrared Spectroscopy of Complexes without Chromophore by Nonresonant Femtosecond Ionization Detection

**ARTICLE** *in* THE JOURNAL OF PHYSICAL CHEMISTRY A · MAY 2012

Impact Factor: 2.69 · DOI: 10.1021/jp303937h · Source: PubMed



**5 AUTHORS**, INCLUDING:

Iker león
Universidad del País Vasco / Euskal Herriko U…
**33** PUBLICATIONS **201** CITATIONS
SEE PROFILE

José Andrés Fernández
Universidad del País Vasco / Euskal Herriko U…
**118** PUBLICATIONS **872** CITATIONS
SEE PROFILE

THE JOURNAL OF PHYSICAL CHEMISTRY A

Article

pubs.acs.org/JPCA

# Mass-Resolved Infrared Spectroscopy of Complexes without Chromophore by Nonresonant Femtosecond Ionization Detection

Iker León, Raúl Montero, Fernando Castaño, Asier Longarte,[‡] and José A. Fernández[‡,*]

Dpto. Química Física, Fac. Ciencia y Tecnología, Universidad del País Vasco-UPV/EHU, B° Sarriena, s/n, 48940 Leioa, Spain

Supporting Information

**ABSTRACT:** Mass-resolved excitation spectroscopic techniques are usually limited to systems with a chromophore, that is, a functional group with electronic transitions in the Vis/UV, with lifetimes from hundreds of picoseconds to some microseconds. In this paper, we expand such techniques to any system, by using a combination of nanosecond IR pulses with nonresonant ionization with 800 nm femtosecond laser pulses. Furthermore, we demonstrate that the technique can achieve conformational specificity introducing an additional nanosecond IR laser. As a proof-of-principle, we apply the technique to the study of phenol$(H_2O)_1$, propofol$(H_2O)_1$ $\gamma$-butyrolactone$(H_2O)_n$, $n$ = 1−3, and $(H_2O)_2$ complexes. While monohydrated phenol and propofol clusters permit a direct comparison with a well-studied system including an aromatic chromophore, $\gamma$-butyrolactone is a cyclic nonaromatic molecule, whose mass-resolved spectroscopy cannot be tackled by conventional techniques. Finally, we further demonstrate the potential of the technique by obtaining the first mass-resolved IR spectrum of the neutral water dimer, a nice example of a system whose ionization-based detection had not been possible to date.

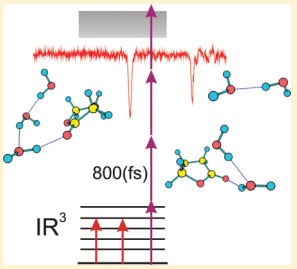


## INTRODUCTION

Mass-resolved excitation spectroscopy (MRES) embraces a number of powerful methods that extend from one color REMPI (resonance-enhanced multiphoton ionization) to very sophisticated double and even triple resonance techniques.[1,2] Such tools, usually employed on molecular beams or supersonic expansions, have provided key spectroscopic information on a broad variety of species with increasing complexity: from few atoms to large biomolecules or molecular clusters.[3] The use of an ionizing probe combined with IR tunable lasers has proved particularly successful, providing a popular method to obtain ground state vibrational spectra. However, the applicability of MRES is limited to systems able to be efficiently ionized by the available radiation sources, which in general requires the existence of a functional group, usually an aromatic ring, acting as a chromophore.

To overcome such constrain, several experimental solutions involving highly efficient multi- or single photon ionizing schemes have been adopted.[4,5] These methods require in general the use of high energy nanoseconds lasers or far UV pulses of complicated generation.[6−8] However, in the last years, the development of ultrashort pulse technology has increased enormously the intensity of the available laser pulses, offering an efficient tool to ionize atoms and molecules. The combination of the high wavelength resolution of traditional nanosecond lasers with such high-intensity sources seems a natural way to expand the capabilities of the mass-resolved frequency-domain techniques. The recent work by Nosenko et al. nicely illustrates this idea, allowing the collection of IR mass-resolved spectra of species with very short-living excited states, by using a fs ionizing probe.[9] In that work, spectra on the OH region of the 1*H*-pyrrolo[3,2-*h*]quinoline/methanol complexes were recorded by depleting the resonant ionization signal generated by the absorption of two 267 nm photons of 300 fs from the third harmonic of a Ti:sapphire laser (Figure 1B), using the short-lived (≪1 ns) excited state of the chromophore as an intermediate state.

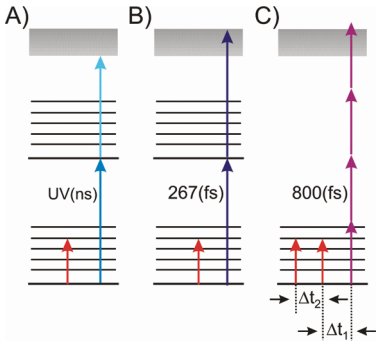


**Figure 1.** Schemes of different mass-resolved double resonance techniques for the collection of ground state IR spectra. (A) IR/UV experiments with resonant ionization by ns UV pulses. (B) Scheme used in ref 9 for the study of species with short lifetimes, based in resonant ionization by 267 nm fs UV pulses. (C) $IR^3$ technique developed in the present work using nonresonant ionization detection by 800 nm fs laser pulses. The additional IR beam provides conformer and mass selectivity.

**Received:** April 24, 2012
**Revised:** May 28, 2012
**Published:** May 29, 2012

Herein, we present a technique, IR/IR$_{fs}^{800}$(abbreviated to IR$^2$), that generalizes the fs ionization detection by using nonresonant multiphoton ionization with an 800 nm fs pulse. As the study shows, high-intensity pulses at this wavelength are able to induce multiphoton absorption, ionizing molecules with an efficiency that depends only on the ionization potential (IP). Mainly due to the nonresonant character of the ionization process, the method can be applied to any system in which the preceding IR absorption causes the disappearance of the species by fragmentation, as it occurs for molecular complexes. Furthermore, a general drawback of all of the techniques based on nonselective ionization is the loss of mass selectivity due to extensive fragmentation processes. In this work, to recover size and molecular selectivity, we combine three IR beams in an IR/IR/IR$_{fs}^{800}$ (IR$^3$) scheme (Figure 1C).

To demonstrate the broad validity of the technique, we apply it to three very different cases (Scheme 1): the monohydrated

**Scheme 1. Molecules Whose Hydrated Clusters Have Been Studied in This Work**

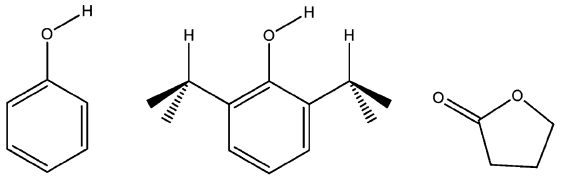


phenol and propofol water clusters, γ-butyrolactone$(H_2O)_n$, $n$ = 1−3 complexes (GBL·W$_n$), and the water dimer. The structure of the H-bonded species resulting from the solvation of phenol and propofol by water has been previously characterized by different spectroscopic methods.[10−12] Comparison of such previous results with those from the application of IR$^2$ allows testing of the capabilities of the methodology on a system easily ionizable through the chromophore's $\pi-\pi^*$ transitions.

On the other hand, GBL is a cyclic species that lacks of strong transitions below 200 nm. Although the −COOR group may induce some absorption in solution around 200 nm depending on the solvent, it cannot be considered as a chromophore in terms of laser spectroscopy in jets. GBL is extensively used in the chemical industry as an odorant and solvent but also as an illegal intoxicant and, therefore, is a controlled or even illegal drug in some countries. When ingested, it is metabolized into γ-hydroxybutyric acid, which is used to treat sleep disorders.[13] GBL is a small molecule, with two oxygen atoms, which may act as proton acceptors when interacting with water. Such an interaction is probably responsible for the high solubility of GBL in water. As we will demonstrate, despite the modest size of the system, several isomers are possible, which give rise to extensive fragmentation upon ionization. However, the use of IR$^3$ allows for recording of the isolated IR spectrum of each species.

As a final example to illustrate the potential of the method, we use it to obtain the IR spectrum of the water dimer. A considerable effort has been devoted to the theoretical and experimental description of this species, as it is the paradigm of the hydrogen bond and the essential building block of water H-bond networks.[14−19] The high IP of water (12.65 eV) and the lack of appreciable absorption below 200 nm have made the mass-detected study of water clusters particularly elusive. Accordingly, although several studies have dealt with the IR spectroscopy of the neutral water dimer,[15,17,20,21] only some of them, namely, molecular beam depletion methods,[22,23] experiments in He droplets,[24] and Argon-mediated population modulated electron attachment spectroscopy,[25] have achieved a partial size-selected IR spectrum of the $(H_2O)_n$, $n$ = 2−6 clusters in the 3300−3800 cm$^{-1}$ region. In this work, we extend the knowledge of the spectroscopy of the water dimer formed in a supersonic expansion by reporting for the first time its mass-selected IR spectrum. This last example illustrates the broad scope of the introduced technique, opening the door to the mass-resolved study of systems whose ionization is not easily achieved by other means.

## METHODS

**Experimental Procedure.** The experiments are carried out in a linear time-of-flight mass spectrometer (Jordan Inc.). The vapor of the samples (97% propofol, Aldrich; 99.5% phenol, Fluka; and >99% GBL, Aldrich) kept at room temperature (except that phenol that was warmed to 60 °C) was mixed with 1−2 atm of He or Ar and expanded through the nozzle of an electromagnetic valve (Jordan Inc.) to form a supersonic expansion. A small amount of water was added to the mixture to form the hydrated complexes. The supersonic jet is collimated by a 1 mm skimmer before entering the ionization region, where it interacts with the ns/fs laser beams. Ultrashort pulses, used as ionizing probes, are generated by a commercial Ti:sapphire oscillator-regenerative amplifier laser system (Coherent) that provides a 1 kHz train of 40 fs pulses centered at 800 nm. A portion of the amplifier output (∼300 μJ) is focused into the ionization region by a 35 cm lens reaching intensities of the order of $10^{13}$ W/cm$^2$. The synchronization of the whole experiment is driven by the clock of the regenerative amplifier, whose 1 kHz trigger output is divided in a delay generator (Stanford SR535) to reach a final 10 Hz sampling rate.

A schematic of the laser arrangement employed in the experiments is shown in Figure 1C. The 800 nm femtosecond ionizing laser is preceded by one or two spatially overlapped IR beams. In the IR$^2$ technique, a single IR beam fired 100−400 ns previous to the femtosecond laser ($\Delta t_1$ in Figure 1C) is scanned along the O−H stretching region of the targeted species. The absorption of the IR radiation, which causes the dissociation of the cluster, is detected as a drop in the ionization signal generated by the fs beam. When conformational selectivity is required, an additional ns IR beam fired at 5 Hz and 100−200 ns previous to the scanning IR laser ($\Delta t_2$ in Figure 1C) depopulates one of the isomers. In this way, because of the active subtraction, a change in the ion signal is only recorded when both IR lasers are resonant with transitions from the same conformer. With this set up, a conformer- and mass-selective IR spectrum is obtained (see refs 2, 26, and 27 for more details on the triple resonance technique).

A commercial Nd:YAG/Dye/$LiNbO_3$ laser system (Quantel Brilliant B/Fine Adjustment Pulsare Pro) with 0.1 cm$^{-1}$ line with and an OPO system (Laser Vision) with a 10 cm$^{-1}$ linewith were used as ns IR laser sources.

It is worthy to say a few words about the particular ionization conditions derived from the use of intense fs laser pulses. At the intensity reached in the experiment, $10^{13}$ W/cm$^2$, different competing mechanisms are involved in the ionization. While multiphoton ionization (six photons of 800 nm are required to ionize phenol or propofol) is predicted to be the dominant


dx.doi.org/10.1021/jp303937h | J. Phys. Chem. A 2012, 116, 6798−6803

process, tunnel and barrier suppression mechanisms also start to be relevant at such intensities.[28] In general, it can be stated that the later mechanisms yield a cleaner ionization,[29] since their high intensities should reduce the fragmentation in the probing process. However, molecular fragmentation has been reported for a molecular system where the barrier suppression is expected to be the main mechanism, which can be related with the complexity of the ionization pathways. This is particularly important for the GBL-water clusters, which seem to undergo a reactive process after ionization, leading to complex fragmentation patterns. Consequently, the intensity of the ionization fs beam has been adjusted in our experiments to maximize the ratio between the parent ion signal and the ionic fragments.

**Calculations.** Data interpretation in the study of GBL-$W_n$ species was guided by the calculations carried out using Maestro and Gaussian 09,[30] running in the computational center of The University of the Basque Country (1300 processors) and in i2BASQUE foundation (1000 processors). Maestro (Schrodinger Inc.) was used for exploration of the conformational landscape, using molecular mechanics (MMFFs force field) and a combination of "large scale-low mode" and Monte Carlo minimization search procedures. A minimum of 100,000 cycles were employed for each species, resulting in 20 isomers for GBL·$W_1$, 23 for the dihydrated species, and 70 for GBL-$W_3$. All of these structures were optimized at M06-2X/6-311++G(d,p) calculation level, imposing no restrictions, resulting in 12, 6, and 33 optimized structures, respectively. In all cases, a normal mode calculation was done to check for the absence of negative frequencies. All of the optimized structures, together with their relative stability in kJ/mol, can be found in the Supporting Information.

## RESULTS AND DISCUSSION

**Phenol and Propofol Hydrated Clusters.** To test the performance of the method, we applied the $IR^2$ technique to the well-studied phenol and propofol monohydrated clusters. Figure 2a shows a comparison between the IR spectra of propofol-$W_1$ in the OH region collected by ionizing with traditional UV ns probe pulses ($IR/UV_{ns}$, upper trace), UV fs pulses at 267 nm ($IR/UV_{fs}$, middle), and nonresonantly with 800 nm fs pulses ($IR/IR_{fs}^{800}$, lower trace). In the case of phenol-$W_1$ (Figure 2b), only the $IR/UV_{ns}$ and $IR/IR_{fs}^{800}$ are shown. Other than the slightly better s/n ratio obtained with the UV ns laser, no important differences are observable in the traces recorded with the three different ionization probes, while at the same time, they agree very well with previous observations.[31] The collected data corroborate the ability of the $IR^2$ to reproduce the known IR spectral features of the clusters. It is worthy to note that the spectra in Figure 2 were recorded in their respective mass channels and that no interference due to fragmentation from higher order clusters is observed.

**GBL Water Clusters.** Once the technique has been demonstrated for systems containing a chromophore, we apply it to the study of GBL hydrated complexes. As mentioned above, the absence of $\pi-\pi^*$ transitions complicates the resonant excitation of such species by UV−vis laser pulses. Figure 3 summarizes the mass spectra of pure GBL and GBL with water, recorded at different experimental conditions using 800 nm fs pulses as ionizing source. In the trace in Figure 3a, collected with no water added to the expansion, the most prominent feature corresponds to the $GBL^+$ mass channel,

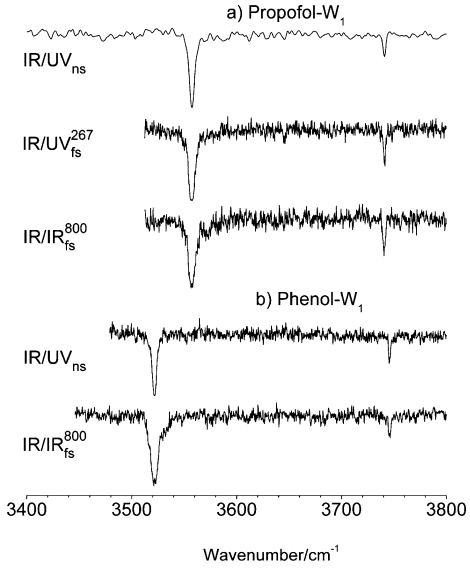


**Figure 2.** (a) Propofol-$W_1$ IR/UV traces obtained using two-color REMPI detection scheme with the ns laser at 36030 $cm^{-1}$ and nonresonant ionization with 267 and 800 nm fs pulses. (b) Phenol-$W_1$ IR/UV traces obtained using ns REMPI at 36350 $cm^{-1}$ and nonresonant ionization 800 nm fs pulses.

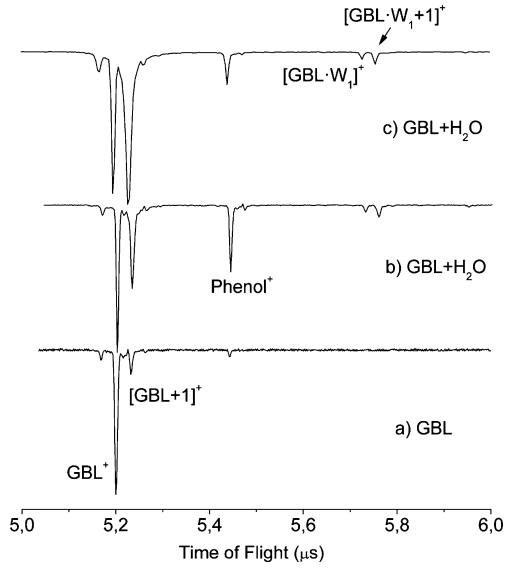


**Figure 3.** Mass spectrum of (a) an expansion of GBL in He, (b) an expansion of GBL/water in He, and (c) the same expansion but adjusting the laser-valve delay to maximize the signal in the $[GBL + 1]^+$ mass channel. For all of the mass spectra, the energy of the 800 nm pulse was adjusted at ∼300 $\mu J$ to obtain the best ratio between GBL signal and molecular fragments.

which is formed after the absorption of 7 photons of 800 nm. The peak at $[GBL + 1]^+$ mass channel accounts for isotopically substituted GBL* species (i.e., mainly with at least one hydrogen replaced by a deuterium or a $^{12}C$ replaced by a $^{13}C$) and for $[GBL + H]^+$ ions produced in the dissociation of GBL-$W_1^+$ clusters (see below), formed due to the presence of water traces in the original sample. A small peak at $[GBL^*\text{-}1]^+$ amu is attributed to the GBL losing a hydrogen atom. Finally, the weak feature around ∼5.4 $\mu$s flight time corresponds to the phenol ion, which is introduced in the system as reference molecule and to assist in the alignment.


dx.doi.org/10.1021/jp303937h | J. Phys. Chem. A 2012, 116, 6798−6803

Spectra 3b,c were recorded after adding a small amount of water. Both traces show an increment of the intensity of the $[GBL\text{-}W_1]^+$, $[GBL+1]^+$, and $[GBL\text{-}W_1 + 1]^+$ mass channels. The last two species are due to a reactive process in the ion that leads to the dissociation of the water molecule. Although the overall reaction can be generically described by

$$GBL(H_2O)_n^+ \rightarrow GBL(H_2O)_{n-1}H^+ + OH \quad (1)$$

the exact mechanism is unclear and should be the subject of further study.

The high efficiency of the process is revealed by the fact that the adjustment of the valve-laser delay permits one to optimize the signal of the protonated species to intensities that overcome those of the nonprotonated ones (see Figure 3c). Such an effect is not observed when water is not added to the expansion. As a final test on the origin of the hydrogen atom, the same experiment was repeated but using methanol as solvent instead of water. The more acidic character of methanol should make it a better proton donor, resulting in a higher amount of protonated species. Figure S1 in the Supporting Information shows the two mass spectra obtained probing a GBL/methanol expansion with fs pulses of 800 nm, after optimizing the experimental conditions to maximize the signal in the [GBL-methanol]$^+$ (lower trace) and [GBL-methanol + 1]$^+$ (upper trace) mass channels. In this system, the signal of protonated GBL·methanol complexes is stronger under all conditions, confirming the origin of the protonated species.

The $IR^2$ spectrum collected at the $[GBL\text{-}W_1]^+$ mass channel is shown in Figure 4a. While only two frequencies, corresponding to the two OH stretches, were expected in this region, at least five features are clearly visible, pointing to the presence of more than one species. To isolate the individual contributions, $IR^3$ experiments probing the transitions at 3535 (Figure 4b) and at 3454 $cm^{-1}$ (Figure 4c) were carried out. Despite the reduced s/n ratio, we can conclude that the trace in Figure 4a results from the sum of the spectra in Figure 4b,c. It is worth to mention that the broader transitions observed in the $IR^3$ trace, particularly in Figure 4b, are likely due to the lower resolution (10 $cm^{-1}$) of the OPO system used as second IR source. This fact precludes the full isolation of some bands originated in different species, as it happens for the doublets around 3520 and 3720 $cm^{-1}$.

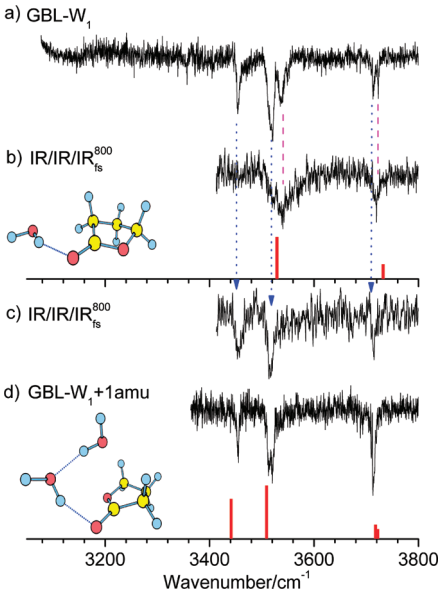


**Figure 4.** (a) $IR/IR_{fs}^{800}$ spectrum obtained integrating $[GBL\text{-}W_1]^+$ mass channel, (b) $IR/IR/IR_{fs}^{800}$ spectrum obtained probing the band at 3535 $cm^{-1}$ with the first IR laser, (c) $IR/IR/IR_{fs}^{800}$ spectrum obtained probing the band at 3454 $cm^{-1}$ with the first IR laser, (d) $IR/IR_{fs}^{800}$ spectrum obtained integrating $[GBL\text{-}W_1 + 1]^+$ mass channel. The sticks represent the calculated frequencies for the structures to which the species are assigned. A correction factor of 0.938 has been applied to the calculated frequencies.

The comparison of the features observed in Figure 4b with those predicted for the most stable calculated geometries (Figures S2 and S3 in the Supporting Information) allows us to unambiguously assign the spectrum to the most stable geometry obtained, in which the water molecule is hydrogen bonded to the carboxylic oxygen of GBL.

Regarding the trace Figure 4c, its origin has to be found in a cluster with different stoichiometry. It mimics the IR spectrum collected by integrating the $[GBL\text{-}W_1 + 1]^+$ mass channel (trace in Figure 4d) that results mainly from the reactive ionization of the $GBL\text{-}W_2$ cluster. Consequently, the transitions in the trace in Figure 4c also correspond to $GBL\text{-}W_2$, which loses a water molecule in the ionization process. To establish the structure of the cluster, the IR spectrum was compared with the predictions from theoretical calculations. Only six conformers were found for this system in the 25 kJ/mol stability window (Figure S4 in the Supporting Information), and in all of them, the two water molecules form a hydrogen bond network, connected to the carboxylic oxygen of GBL. This leads to a very alike set of IR spectra (Figures 4 and S5 in the Supporting Information) that makes difficult the identification of the exact observed conformer. Nevertheless, the calculated structure 2 reproduces better the spacing between bands in the experimental spectrum; therefore, we tend to assign the spectra in Figure 4c,d to such calculated structures. This assignment is further supported by the results obtained using microwave spectroscopy, which unambiguously identify a very similar geometry for the $\beta$-propiolactone$(H_2O)_2$ cluster.[32]

The study also aimed to obtain IR spectra of higher stoichiometry clusters. Despite the very weak signal, it was possible to record the $IR^2$ spectrum in the $GBL\text{-}W_3^+$ mass channel, as shown in the upper panel of Figure 5. The trace is composed of several broad transitions that suggest the existence of more than one species with overlapping spectra. By applying the $IR^3$ technique, it was possible to isolate at least two isomers, assigned to structures in which the water molecules form hydrogen bond networks interacting with the carboxylic oxygen. Those geometries agree again with the one proposed for $\beta$-propiolactone$(H_2O)_3$. The complete set of calculated structures, together with their normal modes, can be found in Figures S6 and S7 in the Supporting Information.

**Water Dimer.** As a final test, we use the $IR^2$ technique to explore the spectroscopy of pure water clusters. Figure 6 shows the IR spectrum of water dimer, recorded in an expansion of He doped with water vapor. Because of the difficulties to isolate the neutral water dimer, the assignment of its IR spectrum, in particular, the position of the bonded OH stretch, has remained controversial for a long time.[33−35] By partially size selecting the water dimer, Buck and Huisken established the occurrence of this transition at 3601 $cm^{-1}$, while they reassigned to the trimer another red-shifted band, erroneously attributed to the dimer.[23] Recently, Kuyanov-Prozument has reported an excellent IR spectrum of water dimer in He droplets using infrared laser depletion spectroscopy.[24] Our mass-selected IR spectrum fully


dx.doi.org/10.1021/jp303937h | J. Phys. Chem. A 2012, 116, 6798−6803

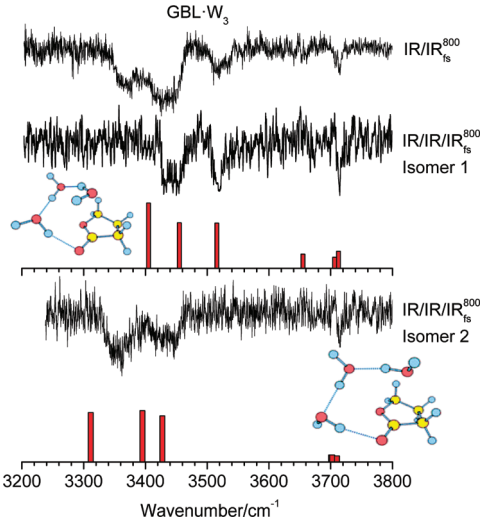


**Figure 5.** IR/IR$_{fs}^{800}$ of GBL-W$_3$ (upper trace). Two isomers are detected using IR/IR/IR$_{fs}^{800}$ (middle and lower traces). The structures to which the two isomers are assigned are also shown, together with their predicted vibrations. A scaling factor of 0.938 was used to correct the simulated spectra for the anharmonicity.

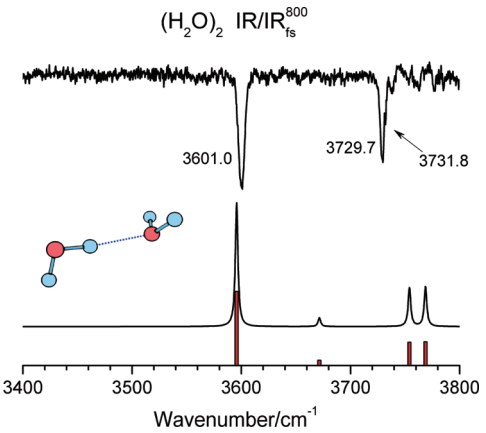


**Figure 6.** IR/IR$_{fs}^{800}$ spectrum of water dimer, recorded using He as buffer gas and 800 nm fs pulses with 300 $\mu$J/pulse, integrating the water dimer mass channel (upper trace). Predicted spectrum for the water dimer at the M06-2X/6-311++G(d,p) level (lower trace). A scaling factor of 0.942 was applied to the simulated spectrum.

agrees with such data and agrees very well with the theoretical calculations at the M06-2X/6-311++G(d,p) level. The transition at 3601 cm$^{-1}$ corresponds to the bonded OH stretching, while the two free OH stretching vibrations almost overlap around 3730 cm$^{-1}$. As in the case of Buck and Huisken and Kuyanov-Prozument and as it frequently happens in clusters involving water molecules, the OH symmetric stretch of the proton acceptor molecules is not observed due to its low intensity, which is predicted to be 14 times weaker than the bonded OH stretch.

Although the extension of the experiment to bigger water clusters seems straightforward, it entails some particularities. The cyclic structures that the clusters with more than two water molecules present undergo dramatic geometry changes upon ionization, involving the ring opening.[36] This fact presumably leads to complicated fragmentation patterns that notably hamper the size-selected detection of the species. The possibility of extracting the IR spectra from fragment channels is currently being explored in our lab.

## CONCLUSIONS

In this work, we introduce a new technique that allows recording mass-resolved IR spectra of molecular aggregates, by combining the wavelength resolution of ns pulses and the ability to induce multiphoton nonresonant ionization of 800 nm fs laser pulses. As a proof-of-principle, we apply the technique to three systems with very different chemical properties. The phenol and propofol monohydrated species are well-studied examples of the solvation of aromatic chromophores. The method faithfully reproduces the data obtained by using ns UV lasers as an ionization source. We also demonstrate the capabilities of the technique by studying the spectroscopy of the $\gamma$-butyrolactone−water system, recording the spectra of its clusters containing up to three water molecules. Comparison of the recorded spectra with DFT calculations allows us to elucidate the geometry of the formed species. A refinement of the technique, consisting of introducing an additional IR laser (IR/IR/IR$_{fs}^{800}$ or abbreviated, IR$^3$), permits recording isomer-selective mass-resolved IR spectra, broadening the scope of the technique, as spectroscopy of more complicated systems can be tackled. Finally, the IR spectrum of water dimer shows the potential application of the method to systems that are not easily ionizable by other means, opening the possibility of achieving mass selectivity in the study of systems of increasing complexity.

We are currently working on a modification that may also allow recording of the spectra of the bare molecule. A combination of photons of different wavelengths or use of a messenger atom technique are some of the options that we are exploring.

## ASSOCIATED CONTENT

### Supporting Information

Calculated structures and their relative energies and predicted spectra and GBL(CH$_3$OH) mass spectra. This material is available free of charge via the Internet at http://pubs.acs.org.

## AUTHOR INFORMATION

### Corresponding Author

*Tel: +34946015387. Fax: +34946013500. E-mail: josea.fernandez@ehu.es. Web: https://sites.google.com/site/gesemupv/.

### Author Contributions

‡These authors share the senior authorship.

### Notes

The authors declare no competing financial interest.

## ACKNOWLEDGMENTS

The research leading to these results has received funding from the Spanish ministry of Science and Innovation-MICINN (Consolider-Ingenio 2010/SAUUL-CSD2007-00013, CTQ2009-14364, and CTQ2010-17749). I.L. thanks the GV for a predoctoral fellowship. Computational resources from the SGI/IZO-SGIker and i2BASQUE were used for this work. Technical and human support provided by the Laser Facility of the SGIKER (UPV/EHU, MICINN, GV/EJ, ESF) is also gratefully acknowledge.

## REFERENCES


(1) Demtroder, W. *Laser Spectroscopy*, 4th ed.; Springer-Verlag: Berlin, 2008.
(2) Shubert, V. A.; Zwier, T. S. *J. Phys. Chem. A* **2007**, *111*, 13283−13286.
(3) Schermann, J. P. *Spectrocopy and Modelling of Biomolecular Building Blocks*; 1st ed. ed.; Elsevier: Amsterdam, 2008.
(4) Heinbuch, S.; Dong, F.; Rocca, J. J.; Bernstein, E. R. *J. Chem. Phys.* **2007**, *126*, 244301.
(5) Fu, H. B.; Hu, Y. J.; Bernstein, E. R. *J. Chem. Phys.* **2006**, *124*, 024302.
(6) Hu, Y. J.; Fu, H. B.; Bernstein, E. R. *J. Chem. Phys.* **2006**, *125*, 114305.
(7) Heinbuch, S.; Dong, F.; Rocca, J. J.; Bernstein, E. R. *J. Chem. Phys.* **2006**, *125*, 154317.
(8) Hu, Y. J.; Fu, H. B.; Bernstein, E. R.. *J. Chem. Phys.* **2006**, *125*, 14310.
(9) Nosenko, Y.; Kunitski, M.; Thummel, R. P.; Kyrychenko, A.; Herbich, J.; Waluk, J.; Riehn, C.; Brutschy, B. *J. Am. Chem. Soc.* **2006**, *128*, 10000−10001.
(10) Kayano, M.; Ebata, T.; Yamada, Y.; Mikami, N. *J. Chem. Phys.* **2004**, *120*, 7410−7417.
(11) Luchow, A.; Spangenberg, D.; Janzen, C.; Jansen, A.; Gerhards, M.; Kleinermanns, K. *Phys. Chem. Chem. Phys.* **2001**, *3*, 2771−2780.
(12) Leon, I.; Cocinero, E.; Millan, J.; Jaeqx, S.; Rijs, A.; Lesarri, A.; Castano, F.; Fernandez, J. A. *Phys. Chem. Chem. Phys.* **2012**, *14*, 4398.
(13) Brunton, L. L.; Lazo, J. S.; Parker, K. L. *Goodman & Gilman's The Pharmacological Basis of Therapeutics*; 11th ed.; McGraw Hill: New York, 2006.
(14) Saykally, R. J. *Abstr. Pap. Am. Chem. Soc.* **2004**, *228*, U535.
(15) Keutsch, F. N.; Braly, L. B.; Brown, M. G.; Harker, H. A.; Petersen, P. B.; Leforestier, C.; Saykally, R. J. *J. Chem. Phys.* **2003**, *119* (17), 8927−8937.
(16) Goldman, N.; Leforestier, C. J.; Saykally, R. J.. *Abstr. Pap. Am. Chem. Soc.* **2003**, *226*, U302.
(17) Huneycutt, A. J.; Saykally, R. J. *Science* **2003**, *299* (5611), 1329−1330.
(18) Keutsch, F. N.; Saykally, R. J. Water clusters. *Proc. Natl. Acad.f Sci. U.S.A.* **2001**, *98* (19), 10533−10540.
(19) Leforestier, C. J.; Braly, L. B.; Fellers, R. S.; Keoshian, C.; Saykally, R. J.. *Abstr. Pap. Am. Chem. Soc.* **2001**, *222*, U186.
(20) Keutsch, F. N.; Cruzan, J. D.; Saykally, R. J. *Chem. Rev.* **2003**, *103*, 2533−2577.
(21) Leforestier, C.; van Harrevelt, R.; van der Avoird, A. *J. Phys. Chem. A* **2009**, *113* (44), 12285−12294.
(22) Huisken, F.; Kaloudis, M.; Kulcke, A.. *J. Chem. Phys.* **1996**, *104*, 17−25.
(23) Buck, U.; Huisken, F. *Chem. Rev.* **2000**, *100*, 3863−3890.
(24) Kuyanov-Prozument, K.; Choi, M. Y.; Vilesov, A. F. *J. Chem. Phys.* **2010**, *132*, 014304.
(25) Diken, E. G.; Robertson, W. H.; Johnson, M. A. *J. Phys. Chem. A* **2004**, *108* (1), 64−68.
(26) Weiler, M.; Bartl, K.; Gerhards, M. *J. Chem. Phys.* **2012**, *136*, 114202−114206.
(27) Leon, I.; Millan, J.; Cocinero, E.; Lesarri, A.; Castano, F.; Fernandez, J. A. *Phys. Chem. Chem. Phys.* **2012**. DOI: 10.1039/c2cp40656j.
(28) Fuss, W.; Schmid, W. E.; Trushin, S. A. *J. Chem. Phys.* **2000**, *112*, 8347−8362.
(29) Vorsa, V.; Kono, T.; Willey, K. F.; Winograd, N. *J. Phys. Chem. B* **1999**, *103*, 7889−7895.
(30) Frisch, M. J.; Trucks, G. W.; Schlegel, H. B.; Scuseria, G. E.; Robb, M. A.; Cheeseman, J. R.; Scalmani, G.; Barone, V.; Mennucci, B.; Petersson, G. A.; Nakatsuji, H.; Caricato, M.; Li, X.; Hratchian, H. P.; Izmaylov, A. F.; Bloino, J.; Zheng, G.; Sonnenberg, J. L.; Hada, M.; Ehara, M.; Toyota, K.; Fukuda, R.; Hasegawa, J.; Ishida, M.; Nakajima, T.; Honda, Y.; Kitao, O.; Nakai, H.; Vreven, T.; Montgomery, J. A., Jr.; Peralta, J. E.; Ogliaro, F.; Bearpark, M.; Heyd, J. J.; Brothers, E.; Kudin, K. N.; Staroverov, V. N.; Kobayashi, R.; Normand, J.; Raghavachari, K.; Rendell, A.; Burant, J. C.; Iyengar, S. S.; Tomasi, J.; Cossi, M.; Rega, N.; Millam, J. M.; Klene, M.; Knox, J. E.; Cross, J. B.; Bakken, V.; Adamo, C.; Jaramillo, J.; Gomperts, R.; Stratmann, R. E.; Yazyev, O.; Austin, A. J.; Cammi, R.; Pomelli, C.; Ochterski, J. W.; Martin, R. L.; Morokuma, K.; Zakrzewski, V. G.; Voth, G. A.; Salvador, P.; Dannenberg, J. J.; Dapprich, S.; Daniels, A. D.; Farkas, O.; Foresman, J. B.; Ortiz, J. V.; Cioslowski, J.; Fox, D. J. *Gaussian 09*, revision A.02; Gaussian, Inc.: Wallingford, CT, 2009.
(31) Watanabe, T.; Ebata, T.; Tanabe, S.; Mikami, N. *J. Chem. Phys.* **1996**, *105*, 408−419.
(32) Sanchez, R. Espectros de rotación en jets supersónicos: Complejos con enlaces de hidrógeno. Ph. Thesis, Universidad de Valladolid, 2005.
(33) Coker, D. F.; Miller, R. E.; Watts, R. O. *J. Chem. Phys.* **1985**, *82*, 3554−3562.
(34) Nelander, B. *J. Chem. Phys.* **1988**, *88* (8), 5254−5256.
(35) Page, R. H.; Frey, J. G.; Shen, Y. R.; Lee, Y. T. *Chem. Phys. Lett.* **1984**, *106*, 373−376.
(36) Barnett, R. N.; Landman, U. *J. Phys. Chem. A* **1997**, *101* (2), 164−169.